Royal Military Academy

Signal and Image Centre

Brussels — Belgium

ERS-1 and ERS-2 scatterometer calibration

Technical report no: RMA-SIC-150204

X. Neyt and A. Elyouncha

June 3, 2015

Contents

Chapter 1

Reference documents

[1] Evert P.W. Attema. Engineering calibration of the ERS-1 active microwave instrumentation in orbit. In *Proceedings of the IGARSS 88 Symposium, Edinburgh, Scotland*, pages 859–862, September 1988.

[2] A. Elyouncha and X. Neyt. A method for cross-comparison of scatterometer data using natural distributed targets: application to ERS-1 and ERS-2 data during the tandem mission. In *Proc. SPIE 8532, Remote Sensing of the Ocean, Sea Ice, Coastal Waters, and Large Water Regions 2012*, October 2012.

[3] A. Elyouncha and X. Neyt. C-band satellite scatterometer inter-calibration. *IEEE Transactions on Geoscience and Remote Sensing*, 51(3):1478–1491, March 2013.

[4] H. Hersbach1, A. Stoffelen, and S. de Haan. Comparison of C-Band scatterometer CMOD5.N equivalent neutral winds with ECMWF. *Journal of Atmospheric and Oceanic Technology*, 27:721–736, April 2010.

[5] N. Manise, X. Neyt, and M. Acheroy. Calibration of the ERS-2 scatterometer in GYRO-LESS mode. In *supl.TIIProc 2004*, volume 68, pages 373–380, September 2004.

[6] N. Manise, X. Neyt, and M. Acheroy. Calibration strategy for ERS scatterometer data reprocessing. In *Proceedings of the SPIE: Remote Sensing of the Ocean, Sea Ice, and Large Water Regions*, volume 5977, pages 88–97, September 2005.

[7] A. Stoffelen. A simple method for calibration of a scatterometer over the ocean. *Journal of atmospheric and oceanic technology*, 16(2):275–282, February 1999.

[8] J. Verspeek, A. Stoffelen, A. Verhoef, M. Portabella, and J. Vogelzang. ASCAT-B ocean calibration and wind product. In *2012 EUMETSAT Meteorological Satellite Conference (2012), Sopot, Poland*, September 2012.

Chapter 2

Calibration methodology

2.1 Calibration over the rainforest

The Amazon rainforest is used to assess the ERS-2/AMI antenna gain pattern [2, 3, 6]. In first approximation, the Amazon forest is characterized by its spatial homogeneity (though not perfectly homogeneous, see masking section), temporal stability and its anisotropy. Thus, the backscatter (sigma nought) over the rainforest only depends on incidence angle. In order to compensate for this incidence angle variation, the sigma nought is converted into gamma nought

$$\gamma^0(\theta) = \frac{\sigma 0(\theta)}{\cos(\theta)} \tag{2.1}$$

where θ is the incidence angle.

A spatial mask can be used to enhance the homogeneity of the rainforest [6]. The mask is built by selecting the data (gamma nought) of which the average value and variance are within $\pm$ 0.25 dB and $\pm$ 0.15 dB respectively. The mask is built by considering the data from the three beams (fore, mid and aft).

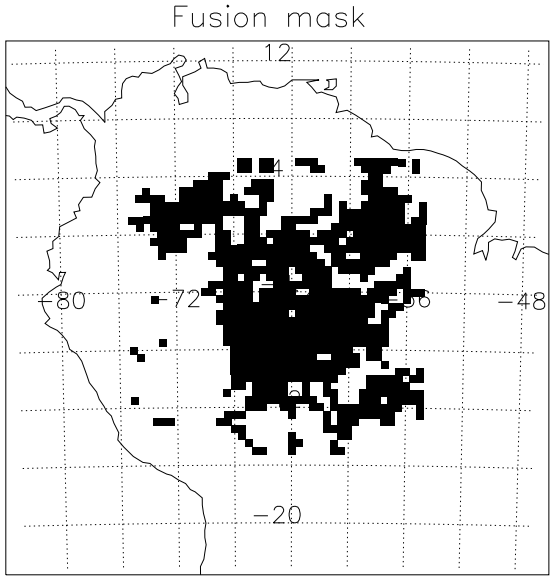

Figure 2.1: Amazon rainforest mask

2.2 Calibration over the ocean

The ocean calibration basically computes the difference (in dB) between the scatterometer measured backscatter $\sigma 0^{meas}$ and the simulated backscatter $\sigma 0^{sim}$ using a GMF and NWP winds [7]. This difference is called here model bias $\beta^m(\theta)$ (see [3] for more details). The model bias $\beta^m(\theta)$ is defined as follows

$$\beta^m_{linear}(\theta) = \frac{\sigma 0^{meas}(\theta)}{\sigma 0^{sim}(\theta)}. \tag{2.2}$$

The GMF used to evaluate the model bias is CMOD5n [4]. The CMOD5na and CMOD6 GMFs are also used for comparison. The CMOD5na and CMOD6 are derived from CMOD5n as follows [8]

$$\sigma 0^{CMOD6}(\theta) = \sigma 0^{CMOD5}(\theta) B_0^{corr}(\theta) \tag{2.3}$$

A first version of B_0^{corr} was issued for CMOD5na

$$B_0^{corr}(\theta) = a0 + a_1\theta + a_2\theta^2 + a_3\theta^3 \tag{2.4}$$

where $a0 = 5.7236425879$, $a_1 = -0.4226930560$, $a_2 = 0.0105605079$, $a_3 = -0.0000864832$.
And a modified version of B_0^{corr} was derived for CMOD6

$$B_0^{corr}(\theta) = a0 + a_1\theta + a_2\theta^2 + a_3\theta^3 + a_4\theta^4 + a_5\theta^5 \tag{2.5}$$

where $a0 = 1.00557711e-02$, $a_1 = 2.63968952e-02$, $a_2 = -1.36487705e-03$, $a_3 = 2.33507248e-05$, $a_4 = 1.20736387e-07$, $a_5 = -4.60930473e-09$.

The NWP winds used as input to the GMF are ERA-interim with 1^0x1^0 spatial resolution and 6 h temporal resolution. Data from the global oceans between latitudes -55^0 and $+65^0$ are used.

Chapter 3

ERS-2 calibration

3.1 Dataset

All the ASPS2.0 data available on the “ftp://ats-merci-uk.eo.esa.int” archive and corresponding to the tandem period are used (590 orbits).

Cycle #	number of orbits	Start date
10	253	1996-Mar-26 001011
11	337	1996-Apr-29 222945

Table 3.1: Calibration dataset

3.2 Calibration results

The results are presented as gamma nought and model bias variation with incidence angle for the calibration over the rainforest and over the ocean respectively. This is assumed to be equivalent to the antenna gain pattern in the elevation plane.

3.2.1 Gamma nought pattern

The gamma nought graphs shown below are obtained by including both ascending and descending passes. Histograms 3.1 and figure 3.2 show, respectively, that the gamma nought has a very narrow distribution and flat pattern. This is expected, since ERS-2 was calibrated over the rainforest assuming a constant gamma model [1, 5, 6].

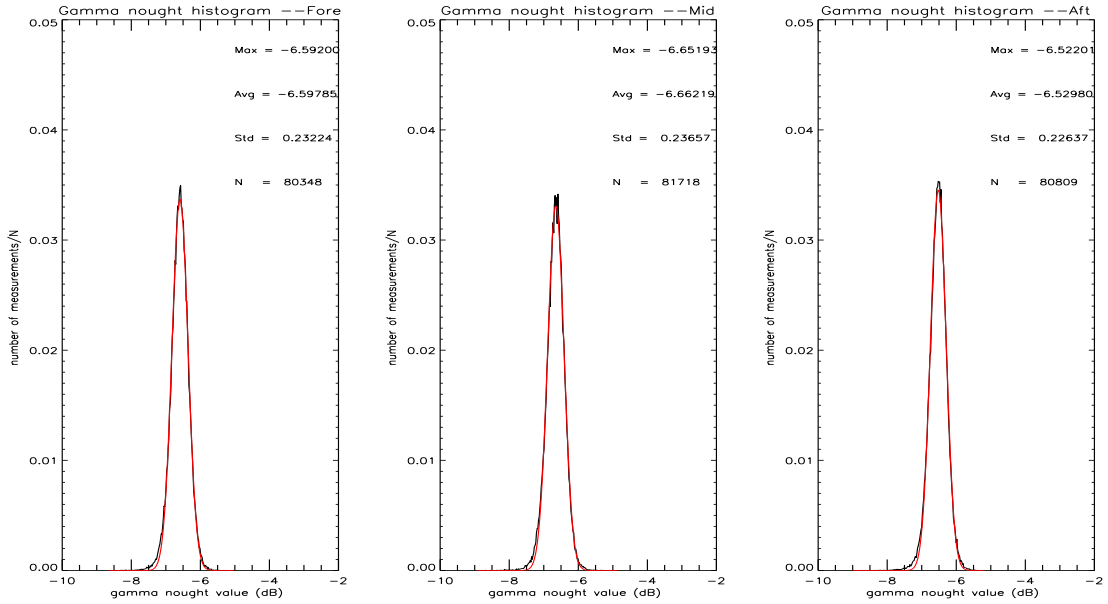

Figure 3.1: Gamma nought histogram - Red: Gaussian fit

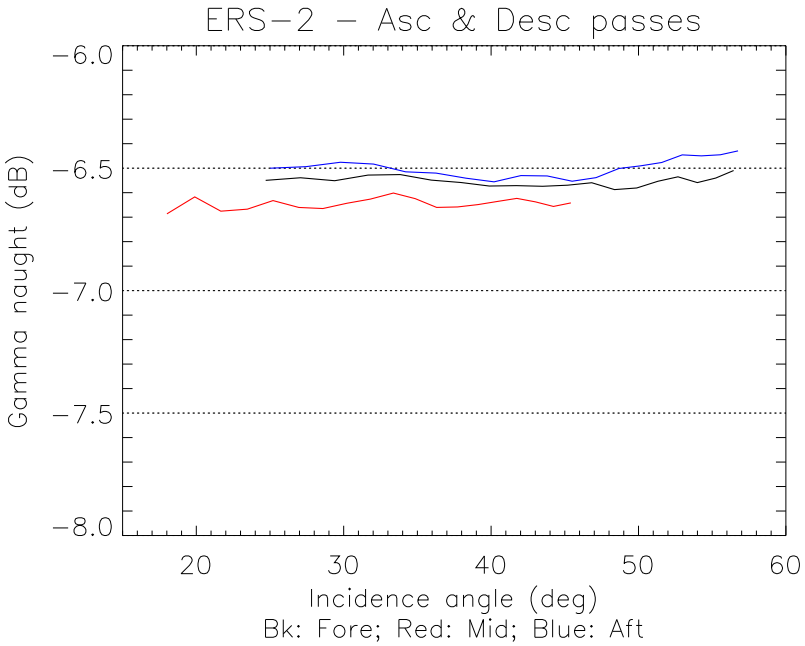

Figure 3.2: Gamma nought

3.2.2 NWP Ocean Calibration (NOC)

The model bias relative to CMOD5n is shown as a function of incidence angle for the three beams. For comparison the CMOD5na [8] *model bias* (green curve) is also shown in figure 3.3. It can be noted that there are relatively large differences, at near and far range, between CMOD5na and the CMOD5n.

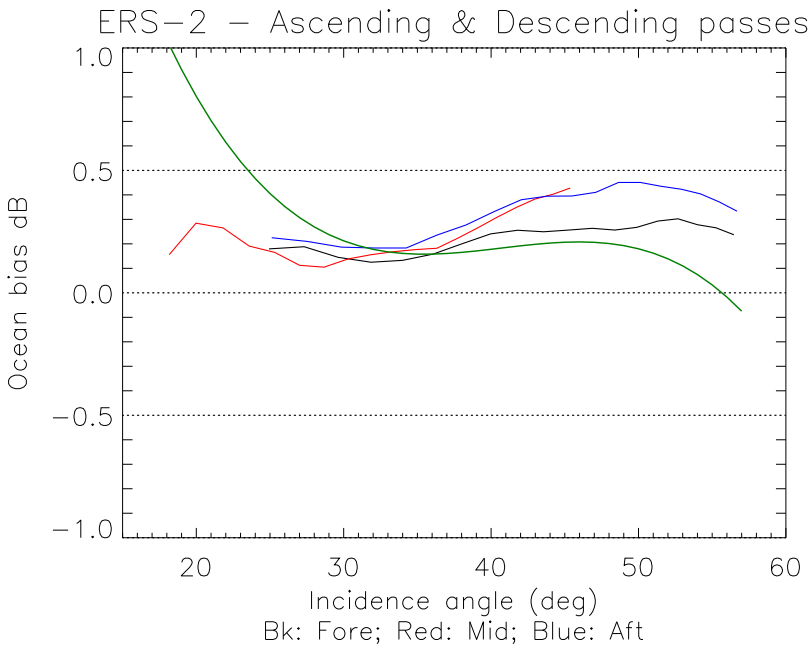

Figure 3.3: Model bias relative to CMOD5n - Green curve: CMOD5na model bias wrt CMOD5n

3.2.3 Application of CMOD5na model bias correction to the rainforest data

In this section, the CMOD5na model is considered as GMF instead of CMOD5n. Correction coefficients are computed from the NOC model bias of ERS-2 data using CMOD5na as GMF (figure 3.4). In order to assess the effect on gamma nought, these correction coefficients are applied to sigma nought. Finally, the gamma nought over the rainforest is computed using the corrected sigma nought as described in section 2.1. It is noted, from figure 3.5, that the gamma nought pattern exhibits a decreasing trend with incidence angle.

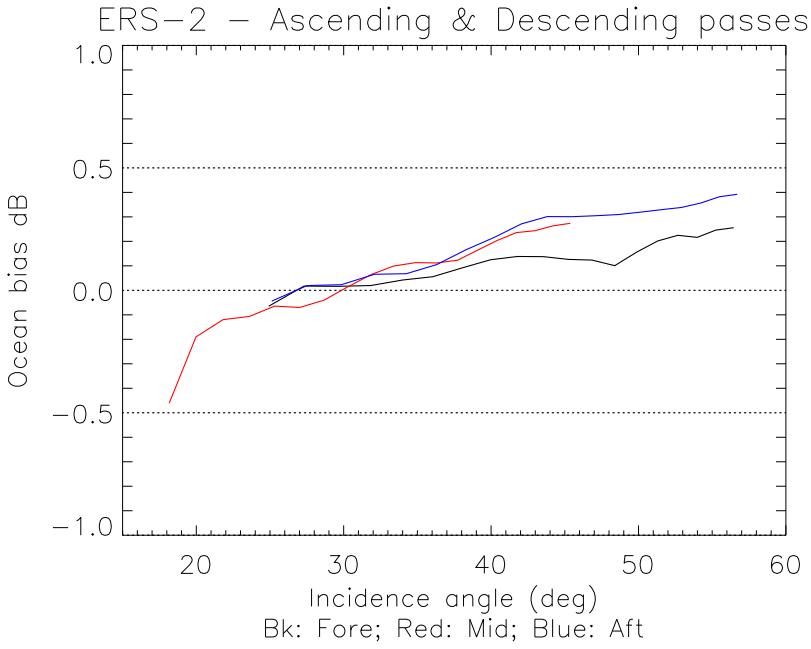

Figure 3.4: Model bias relative to CMOD5na

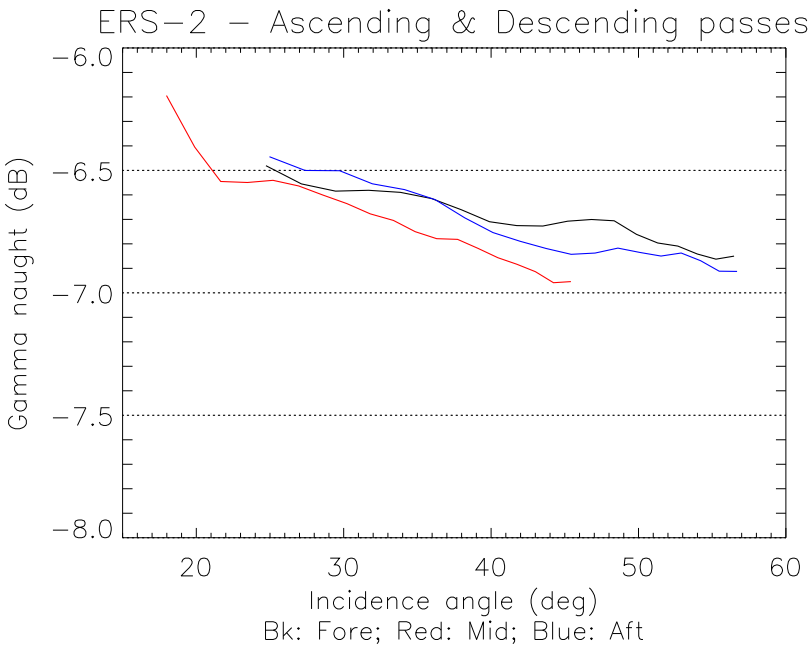

Figure 3.5: Gamma nought obtained after subtraction of the model bias relative to CMOD5na from the sigma nought

Chapter 4

ERS-1 calibration

4.1 Dataset

Cycle #	number of orbits	Start date
155	501	1996-Mar-24 225407
156	501	1996-Apr-29 222945

Table 4.1: Calibration dataset

4.2 ERS-1 gamma nought over the rainforest

Figure 4.1 shows the averaged gamma nought over the rainforest as a function of incidence angle. The gamma patterns are slightly decreasing at high incidence angles.

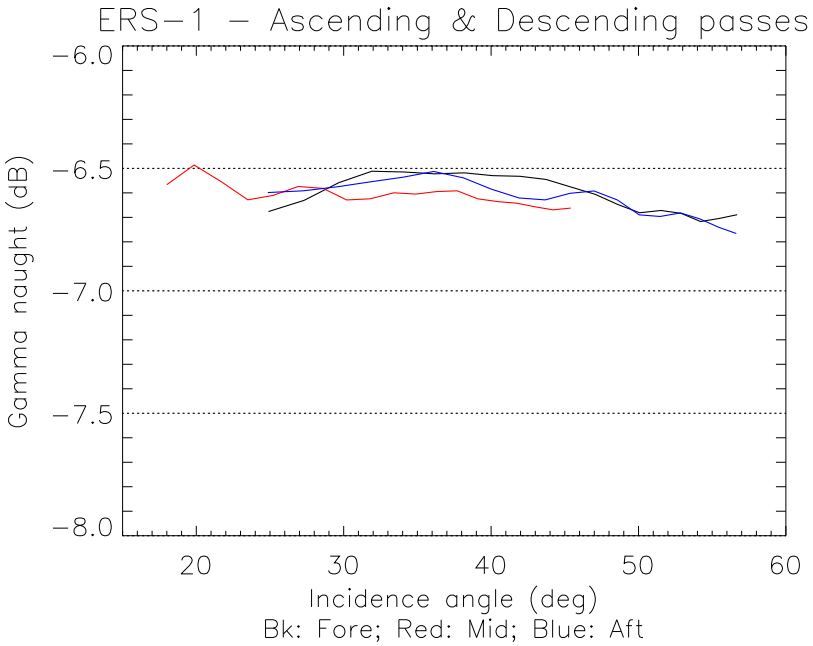

Figure 4.1: Gamma nought - Fore beam - Red: ERS-1, Blue: ERS-2, Black: bias

4.3 ERS-1 NOC

The model bias is computed with respect to CMOD5n GMF. CMOD6 (adapted to ERS low incidence angles) is also shown. A better agreement than CMOD5na with ERS data is noticed, which is expected as the CMOD5na was modified to decrease the bias at low incidence angles.

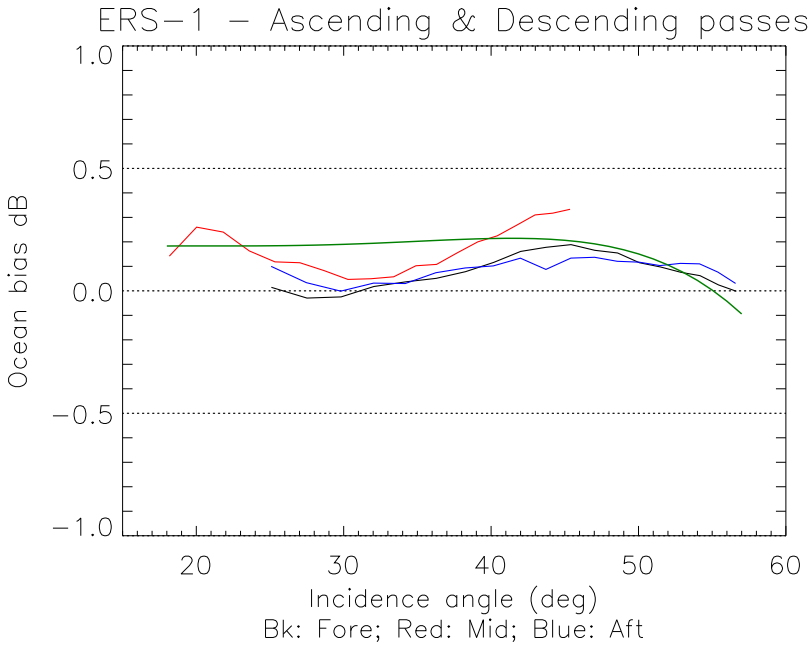

Figure 4.2: Model bias with respect to CMOD5n, Green curve: CMOD6-CMOD5n

Chapter 5

ERS-1/ERS-2 Cross-calibration

5.1 Methodology

The objective of this work is to compute cross-calibration coefficients between ERS-1 and ERS-2 scatterometers. The main underlying assumption of the method is that differences in measured σ_0 are due to differences in antenna gain.

The cross-calibration is a two-step routine:

1. A *model bias* β^m is computed by comparison of the measured ${\sigma_0}^{meas}$ and the simulated ${\sigma_0}^{sim}$

$$\beta^m(\theta,b) = E[\sigma_0(\theta,b)^{meas}]/E[\sigma_0(\theta,b)^{sim}]$$

   where θ and b are the incidence angle and the antenna number respectively. $\sigma_0(\theta,b)^{sim}$ is computed using empirical models (Constant gamma, CMOD5, sea ice model).

2. The *bias* β is computed by comparison of the *model bias* of scat1 and the *model bias* of scat2

$$\beta(\theta,b) = \beta^{m,scat1}(\theta,b)/\beta^{m,scat2}(\theta,b)$$

Since the inter-comparison is performed WVC by WVC, the bias is a function of incidence angle (elevation angle) or the Wind Vector Cell (across-track number). As nominal products are used here, the inter-comparison provides, for each antenna, 19 calibration coefficients.

Herein, the bias β is equal to the difference (ERS-1 - ERS-2). The models are not taken as reference in the absolute sense. In the case rainforest cross-calibration, the model is very simple i.e., constant gamma of -6.5 dB.

Finally, the antenna gain used in normalization function is corrected by the β function and this correction is implemented in the scatterometer processor. Finally, ERS-1 EWIC data are reprocessed using the new synthesized antenna gain pattern.

5.2 Dataset

SAT	Start date	End date	Data format	Data source
ERS-1 (level 0)	26/03/1996	29/04/1996	EWIC	SCIROCCO (ftp://scirocco.sp.serco.eu)
ERS-1 (level 1)	26/03/1996	29/04/1996	CCSDS	IFREMER (ftp://ftp.ifremer.fr/ifremer)
ERS-2 (level 1)	26/03/1996	29/04/1996	ASPS2.0	ESA (ftp://ats-merci-uk.eo.esa.int)

Table 5.1: Calibration dataset

5.3 Calibration results

The results are presented as *model bias* and *bias* variation with incidence angle for the calibration over the rainforest. This is assumed to be equivalent to the antenna gain pattern in the elevation plane.

5.3.1 Cross-calibration bias over rainforest - before reprocessing

Figures 5.1, 5.2 and 5.3 depict the *model bias* (in red and blue) and the *bias* (in black) for the fore, mid and aft beams respectively. The bias is generally small (within 0.15 dB) except for the aft beam witch reaches 0.2 dB at far swath.

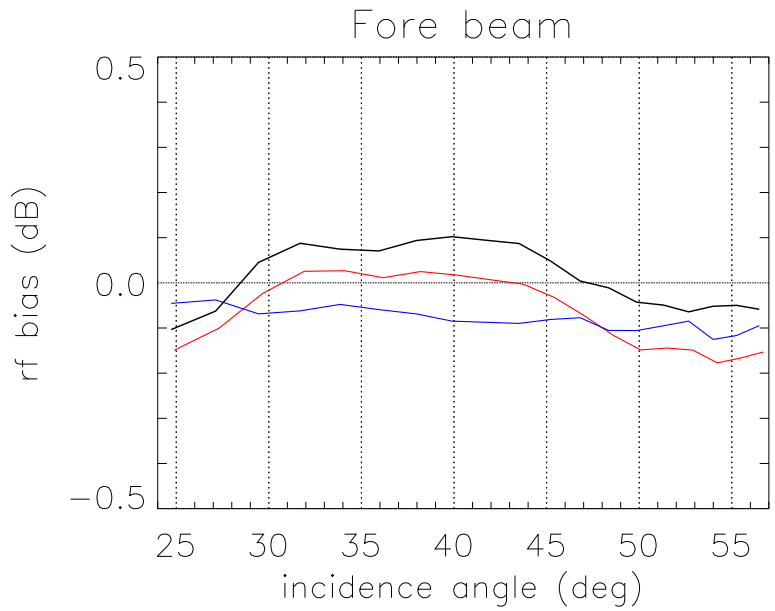

Figure 5.1: Gamma nought bias - Fore beam - Red: ERS-1, Blue: ERS-2, Black: bias

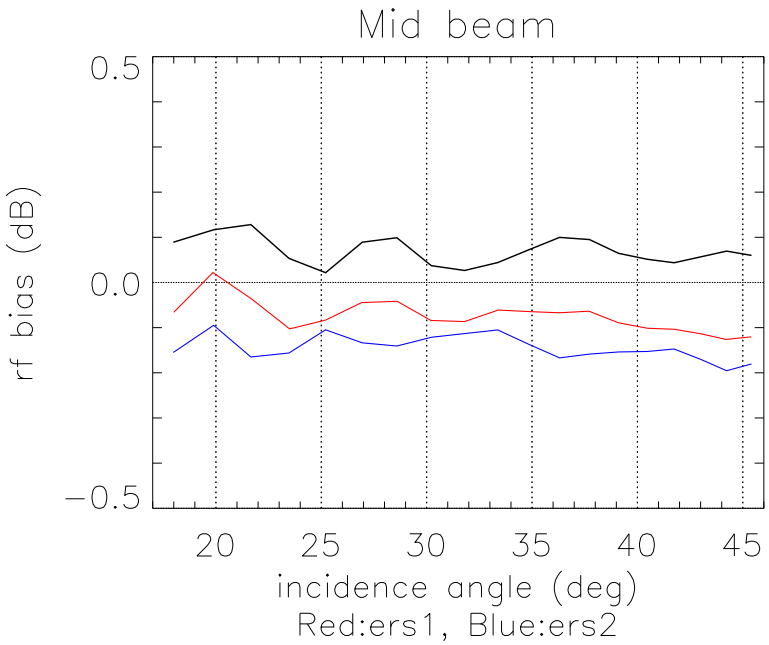

Figure 5.2: Gamma nought bias - Mid beam - Red: ERS-1, Blue: ERS-2, Black: bias

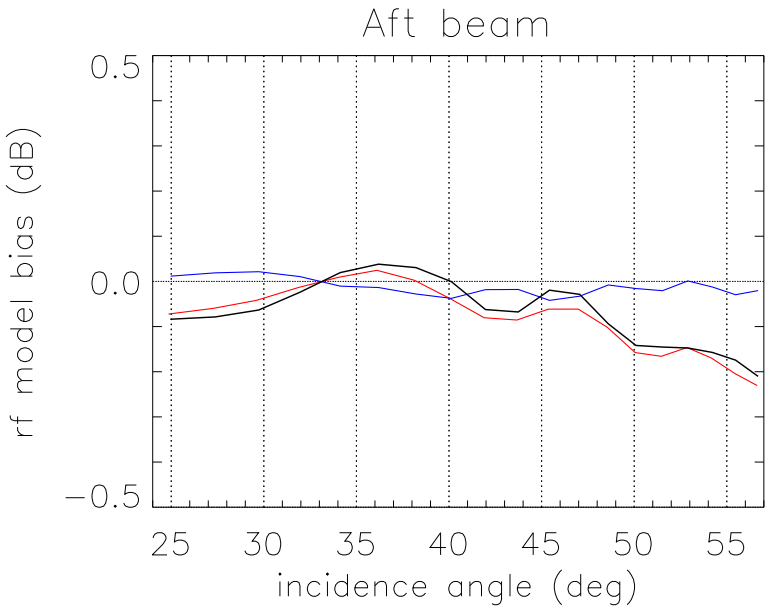

Figure 5.3: Gamma nought bias - Aft beam - Red: ERS-1, Blue: ERS-2, Black: bias

5.3.2 ERS-1 gamma nought pattern after reprocessing

Figure 5.4 depicts the gamma nought pattern of the three beams after ERS-1 re-processing. ERS-2 gamma pattern is also shown aside for comparison. As expected, the two scatterometers have very similar patterns. Note that, now both ERS-1 and ERS-2 show and inter-beam bias between side and mid beam which was less marked in ERS-1 (see figure 4.1).

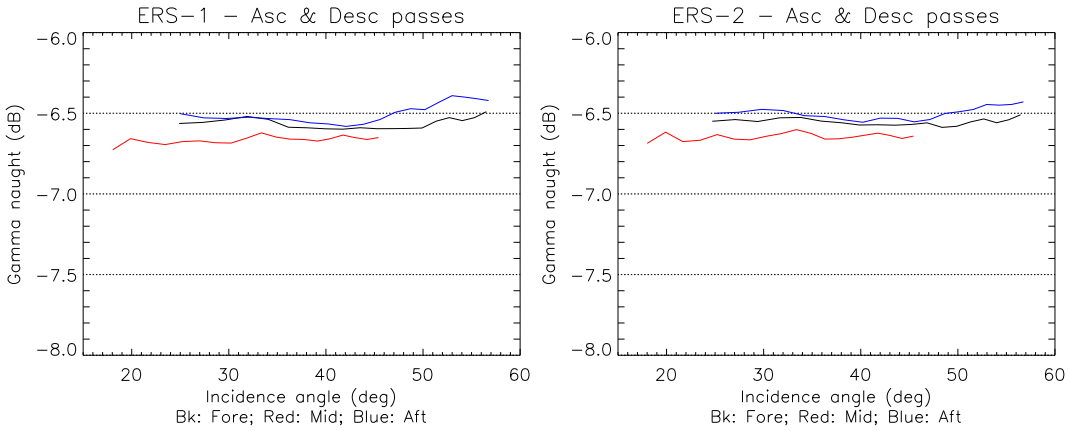

Figure 5.4: Gamma nought - Black: Fore, Red: Mid, Blue: Aft

5.3.3 Cross-calibration bias over rainforest - after reprocessing

After re-processing of ERS-1 EWIC data, a comparison of the produced ASPS2.0 is performed with ERS-2 over the rainforest to assess the cross-calibration. Figures 5.5, 5.6 and 5.7 depict the *model bias* (in red and blue) and the *bias* (in black) for the fore, mid and aft beams respectively, using reprocessed ERS-1 data. The bias is generally negligible (within 0.03 dB) except for the aft beam which reaches a maximum of 0.05 dB.

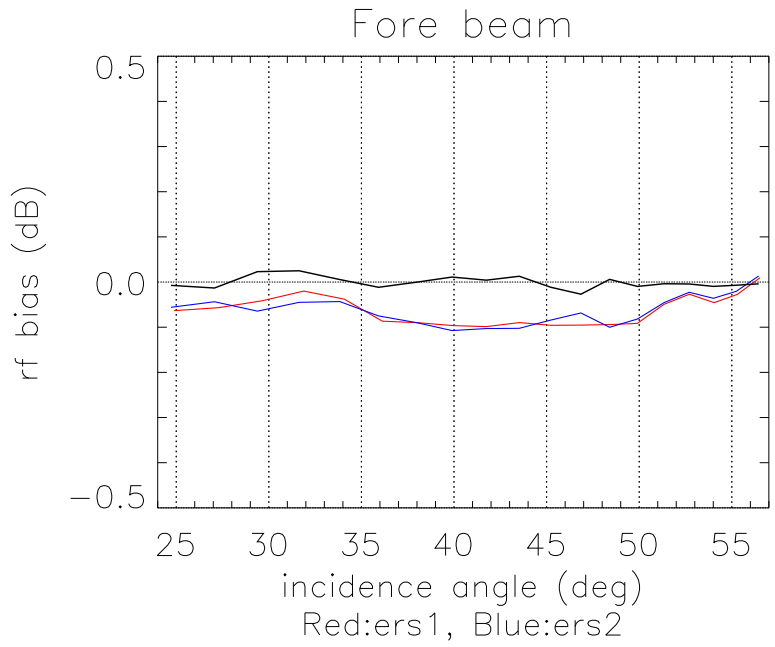

Figure 5.5: Gamma nought bias - Fore beam - Red: ERS-1, Blue: ERS-2, Black: bias

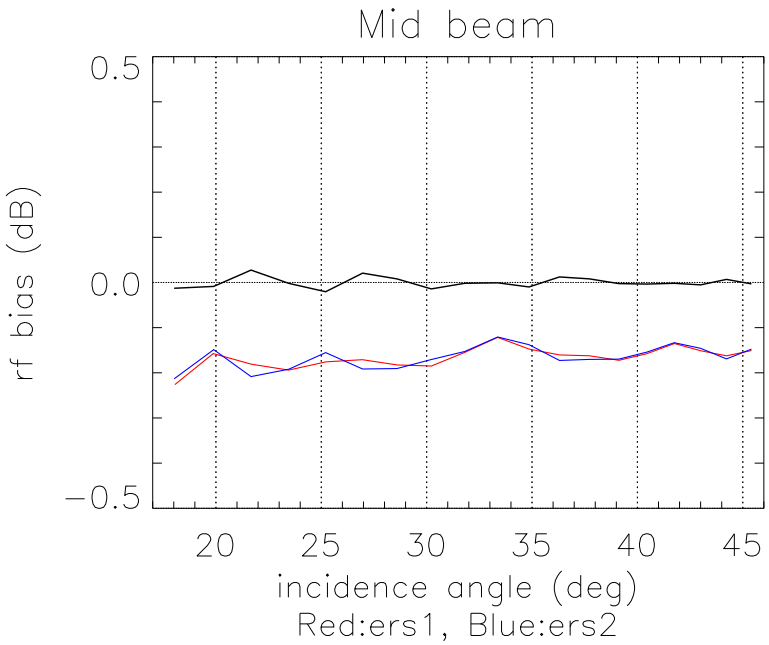

Figure 5.6: Gamma nought bias - Mid beam - Red: ERS-1, Blue: ERS-2, Black: bias

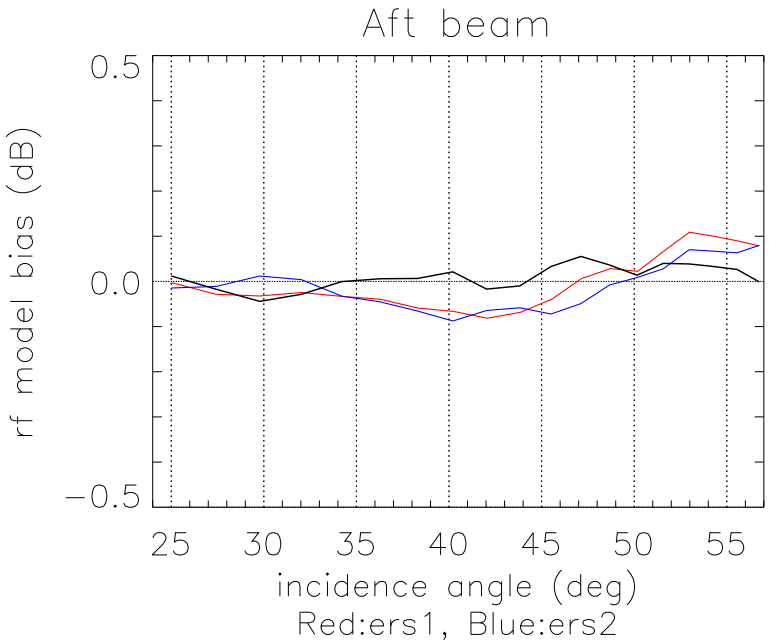

Figure 5.7: Gamma nought bias - Aft beam - Red: ERS-1, Blue: ERS-2, Black: bias

5.4 Effect of CMOD6 calibration on gamma nought pattern

The corrections relative to CMOD6 are applied to ERS-1 backscatter. The gamma nought is computed from the modified backscatter. Figure 5.8 shows the gamma nought after the correction. After CMOD6 correction, the gamma pattern is decreasing at high incidence angle.

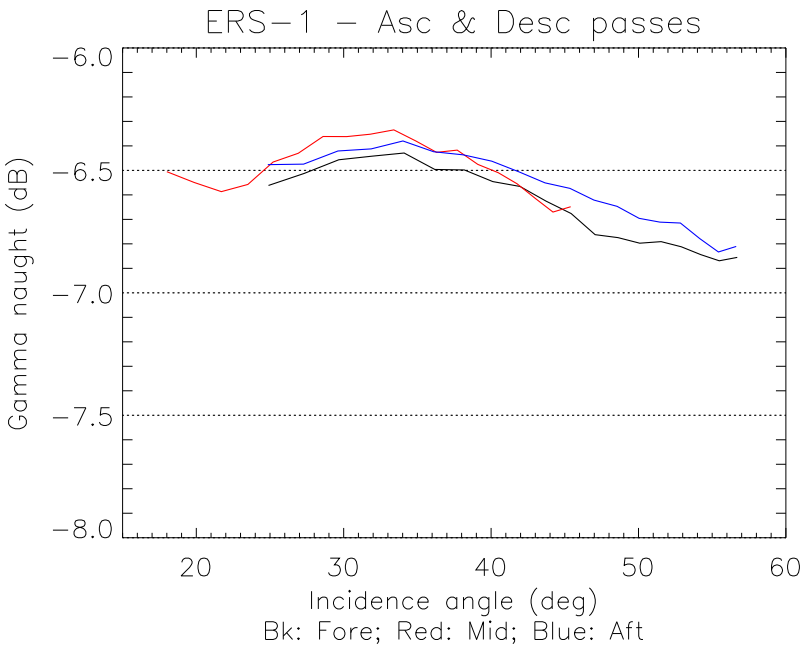

Figure 5.8: Gamma nought - after CMOD6 correction

5.5 Conclusions

For ERS-1 calibration, two calibration strategies are possible

- The strategy implemented in this report maintains the assumption of the constant gamma nought over the rain forest and ERS-2 is used to provide the absolute calibration reference.
- A sample of ERS-1 EWIC data (cycle 155) was reprocessed based on the correction derived from the comparison with ERS-2. After reprocessing, the bias between the two scatterometers is negligible (within 0.03 dB), for Aft beam it is slightly higher with a maximum of 0.05 dB.
- Another possible strategy consists in calibrating using NOC with CMOD6 as GMF. The advantage of this strategy is that the same wind model would then be used for ERS and ASCAT.